

Bruce K. Gale
Merugu Srinivas

Department of Mechanical
Engineering,
University of Utah,
Salt Lake City, UT, USA

Cyclical electrical field flow fractionation

Cyclical electrical field flow fractionation (Cy/EIFFF) is demonstrated in a standard electrical field flow fractionation (EIFFF) channel for the first time. Motivation for the use of alternating current (AC) fields in a traditionally direct current (DC) technique are discussed. The function of the system over a wide range of operating conditions is explored and challenges associated with various operating conditions reported. Retention of polystyrene nanoparticle standards is accomplished and the effect of varying parameters of the applied field, such as voltage and frequency, are explored. The first separations using this technique are demonstrated. The experimental results are compared to analytical models previously reported in the literature. The general trend of the experimental results is similar to those predicted in theoretical models and possible reasons for discrepancies are elucidated. Suggestions are made for improving the separation and analysis method, and possible applications explored.

Keywords: Cyclical fields / Electrophoretic mobility / Field flow fractionation

DOI 10.1002/elps.200410296

1 Introduction

1.1 General aspects

Field flow fractionation (FFF), a family of separation techniques that rely on the laminar flow profile in thin channels, has now been around for over 30 years [1]. One member of this family, electrical field flow fractionation (EIFFF), was one of the first subtypes to be demonstrated [2], but has lagged far behind some of other subtechniques, such as flow, thermal, and sedimentation FFF, in the past three decades. Only in the last 10 years has interest in EIFFF been revived with the development of new instrument designs [3] and miniaturized versions [4]. Still, EIFFF has several limitations that have slowed its development including the static nature of the applied electric field that quickly generates polarization layers. Accordingly, the actual electric field experienced by particles suspended in EIFFF channels (referred to as the effective field) is typically less than 3% [5] of the applied electric field (calculated using the applied voltage divided by the thickness of the channel) and is often less than 1% [3, 6]. Retention in EIFFF is based on the ratio between the electrophoretic mobility and the diffusion coefficient, making it difficult to measure either parameter independently.

Correspondence: Dr. Bruce K. Gale, University of Utah, Department of Mechanical Engineering, 50 S. Central Campus Drive Room 2110, Salt Lake City, UT 84112-9202, USA

E-mail: gale@eng.utah.edu

Fax: +801-585-9826

Abbreviations: **AC**, alternating current; **CY/EIFFF**, cyclic electrical field flow fractionation; **DC**, direct current; **DI**, deionized; **RC**, resistive/capacitive

Two basic solutions have been suggested for the problems of polarization layers and the inability to separate diffusion coefficient and electrophoretic mobility. The first uses isoelectric focusing (IEF), which separates particles based on isoelectric point instead of electrophoretic mobility [7–9]. The second, which will be the focus of this paper, uses oscillating or cyclical applied fields, still relies on electrophoretic mobility, and has recently been reported by our group [10, 11] and others [12]. Recent work has focused on the implementation of pulsed (non-symmetric) fields in microscale EIFFF systems [12], while we have primarily been interested in purely cyclical fields in macroscale systems. Neither of these systems have been adequately characterized with respect to the theory for cyclical field flow fractionation (CyFFF) originally presented by Giddings in 1986 [13] and extended and demonstrated in gravitational FFF in 1988 [14]. A simulation of cyclical electrical field flow fractionation (Cy/EIFFF) was published by Stevens in 1990 [15], but the technique was never demonstrated until recently [10–12]. A major practical limitation of these important papers by Giddings and Stevens is that they do not take into account the polarization layer effects found in solid-wall EIFFF channels, since these channels had not been developed when these papers were published. Several other investigators have reported using oscillating electric fields in flow-based separation systems [16–20] but the complexity of the systems is substantial and operation sufficiently different that they will not be further discussed here.

Cy/EIFFF was slow to be demonstrated for several reasons. Early EIFFF systems were unreliable due to the use of membranes as channel boundaries [2]. More recent instrument designs developed in 1993 by Caldwell [3]

used solid electrodes as the channel walls, which eliminated some of the consistency problems, but introduced the polarization problem. This configuration also generates a system that resembles a large parallel plate capacitor. Associated with this capacitance is a large time constant for electrical equilibrium in the system, which was found to be over 40 s [21] for a typical EIFFF system. This slow response time, along with issues related to effective fields, may have discouraged EIFFF practitioners from attempting the use of cyclical fields.

The recent advent of microscale systems with their smaller time constants [4, 6, 22] presented a more likely candidate for the use of cyclical electrical fields, and Lao *et al.* [12] demonstrated just such a system. But as the results will show, the theory clearly indicates that Cy/EIFFF should work equally well with normal, large-scale systems. Accordingly, this work will report on the theory associated with Cy/EIFFF, the measurement of basic electrical parameters in an EIFFF system to enable optimal separations, and then the retention of particles using cyclical electric fields in an FFF channel.

1.2 Theory

1.2.1 Basic CyFFF concepts

The basic theory for CyFFF was introduced by Giddings and co-workers [13, 14], and the reader is referred there for details related to this work. A brief review of the critical components is appropriate here. In FFF, an external field is applied across a thin channel containing a pressure-driven carrier solution as shown in Fig. 1. The pressure-driven flow generates a parabolic velocity profile. A perpendicular field is applied to control the location of particles in the flow, thereby controlling the relative rate that particles of interest travel down the channel. The retention ratio, R , is defined as the ratio of average particle velocity in the z -direction, $\overline{v_p}$, and average carrier velocity, $\langle v \rangle$

$$R = \frac{\overline{v_p}}{\langle v \rangle} \quad (1)$$

The retention ratio, which can be experimentally measured, is the primary tool for understanding the function and operation of FFF and similar chromatography systems. In cyclical FFF R can be correlated to a dimensionless retention parameter, λ_0 which is given for operation under a square wave electric field by [13]

$$\lambda_0 = \frac{\mu E_0 \tau_c}{2w} \quad (2)$$

where μ is the electrophoretic mobility of the particles, E_0 is the effective magnitude of the varying electric field, τ_c is

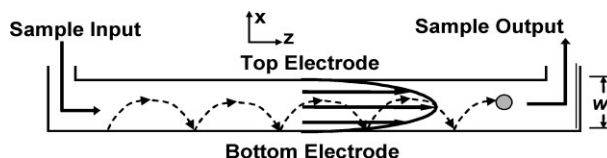


Figure 1. Diagram of a Cy/EIFFF system showing the general configuration of the system, the electrodes for application of the electric fields, the path a particle might take, and the laminar flow profile of the carrier in the channel.

the period of the field oscillation, and w is the electrode separation distance. When $\lambda_0 \geq 1$, the particles subject to the oscillating field will completely traverse the channel before moving back towards the original wall. Thus, λ_0 can be used to divide the operation of Cy/EIFFF into two modes. R depends on the operational mode of particles in the channel. Mode I (as defined by Giddings [14]) occurs when particles do not traverse the channel, so R is given by

$$R = 3\lambda_0 \left(1 - \frac{2\lambda_0}{3}\right) \quad \lambda_0 \leq 1 \quad (3)$$

Mode III occurs when particles traverse the channel and stop at the far wall. In mode III, R is given by

$$R = \frac{1}{\lambda_0} \quad \lambda_0 \geq 1 \quad (4)$$

These two functions connect at $\lambda_0 = 1$ to create a continuous function. Mode II occurs at the point $\lambda_0 = 1$ and can be represented by either model. Note that the only particle characteristic that is important for retention is the electrophoretic mobility.

1.2.2 Electrical effects

The electric field or potential gradient experienced by particles in EIFFF is not the conventional ratio of the applied voltage and distance, but is a complex function of the system geometry, carrier properties, electrode material, and the applied voltage. Most of the applied voltage during direct current (DC) operation is dropped across the electrode-carrier interface and the polarization layer between the electrode and the bulk carrier solution. Thus, the effective electrical field experienced by particles in EIFFF channels is much less than expected (<10% of the applied electric field) [3, 5, 22]. Since the magnitude of the effective field in the channel as a function of frequency is not obvious, a close look at the electrical parameters of an EIFFF channel is required.

Circuit model: The EIFFF channel can be modeled as an electric circuit as shown in Fig. 2 [21, 22]. In this model, the polarization layer at each electrode is represented as a parallel plate capacitor of capacitance C_{DL} in parallel

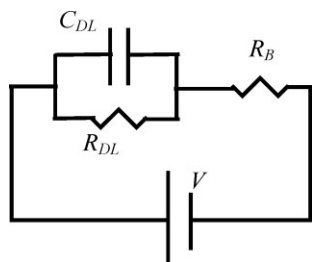


Figure 2. Simple circuit model of EIFFF channel

with an interface resistance R_{DL} . The “effective potential” in the channel is identified as the potential drop across the bulk resistance R_B , since the bulk of the channel is where the particles of interest will be found. Using basic electronics principles, one can obtain the effective field from the model and represent it by

$$E_0 = \frac{VR_B}{w} \sqrt{\frac{1 + (2\pi f R_{DL} C_{DL})^2}{(R_B + R_{DL})^2 + (2\pi f R_B R_{DL} C_{DL})^2}} \quad (5)$$

where V is the applied voltage and f is the frequency of the applied field in Hertz. The frequency is equivalent to $1/\tau_c$.

As with all electric circuits dominated by capacitance, as the frequency of the applied voltage increases, the current in the circuit increases. The current is especially important in EIFFF systems as the effective electric field strength experienced by particles in the channel has been shown to be proportional to the measured electrical current [3, 6]. Conceptually, there is another effect that will also contribute to an increase in the effective field experienced by particles in the channel. If the field is reversed at higher and higher rates, the ions in the carrier cannot shift their positions with the reversal of fields, and a significant polarization layer is unable to develop, effectively reducing the capacitance. Thus, the capacitance in this system will also be a function of time in a DC field and possibly of frequency in an alternating current (AC) field, though that dependence will not be modeled here.

The important question to ask at this point is: At what frequency does the effective field match the applied field? This question can be answered if the electrical parameters of the FFF channel are known. Accordingly, the electrical parameters of the EIFFF channel will be measured and the effective field estimated.

2 Materials and methods

2.1 EIFFF system

The EIFFF system used in this work consists of a syringe pump (Model 100 with 60 mL syringe; KD Scientific, New Hope, PA, USA), power supply (Model E3630; Agilent,

Waldbronn, Germany), digital multimeter (34401A; Hewlett-Packard, Palo Alto, CA, USA), and computer in addition to a traditional EIFFF channel. The EIFFF channel used for all the experiments was 64 cm long, 2 cm wide, and 178 μm deep, and is identical to that used in previous publications [3, 21]. Three carrier solutions were used: 18 M Ω deionized (DI) water, 5 μM Na₂CO₃ solution, and 50 μM Na₂CO₃ solution. Fresh DI water was used for most experiments, and it was stored in a closed container to limit contamination by atmospheric carbon dioxide.

2.2 Channel electrical parameters

The electrical parameters of the channel depend on the carrier used. Therefore, the electrical parameters of the channel were measured for all carriers employed in the experiments based on the equivalent circuit model presented earlier. The technique used to measure the equivalent circuit parameters of the EIFFF channel is similar to that reported previously in the literature [21].

Using basic electrical theory, if a step voltage of magnitude V is applied across the electrodes of an EIFFF system, then the current in the circuit is given by

$$i = \frac{V}{R_B + R_{DL}} \left(1 + \frac{R_{DL}}{R_B} e^{-t/\tau} \right) \quad (6)$$

The resistive/capacitive (RC) time constant, τ , of the circuit equivalent model of the EIFFF channel is given by

$$\tau = \frac{R_B R_{DL} C_{DL}}{R_B + R_{DL}} \quad (7)$$

From Eq. (6) we can deduce that the current in the circuit initially at time $t = 0$ would be

$$i = \frac{V}{R_B} \quad (8)$$

The value of the current decreases exponentially after this time and nearly saturates after five time constants at

$$i = \frac{V}{R_B + R_{DL}} \quad (9)$$

Observations of initial current, saturated current, and time constant give three equations with the variables R_B , R_{DL} , and C_{DL} . Solving these equations, the electrical parameters of the EIFFF system are determined. Once the electrical properties of the channel are determined, the effective field is calculated from Eq. (5) and is used to estimate the elution time of particles in the FFF channel and to optimize a given experiment.

2.3 Cy/EIFFF retention and separations

The experimental setup used for retention and separation experiments is analogous to the traditional EIFFF setup, with the only change being the power source. To generate the cyclical fields needed in Cy/EIFFF, the DC source was replaced with a signal generator (HP-33120A). A UV absorbance detector (Model 500; Lab Alliance, State College, PA, USA) was used to monitor particle elution. A 10 μL Hamilton syringe was used for the injection of sample and 1.0 μL samples were used in all experiments. Retention experiments were performed using standard polystyrene particles of 110 nm and 160 nm diameter (Bangs Laboratories, Fishers, IN, USA) diluted to 1% of their original concentration in DI water. The surfaces of some of particles were carboxylated to modify the electrophoretic mobilities of some particles of the same size. Demonstration separations were performed using 209 nm carboxylated polystyrene particles and 200 nm silica particles. Overall, the electrophoretic mobilities ranged from 2×10^{-5} to 1×10^{-4} $\text{cm}^2/\text{V}\cdot\text{s}$ as measured using a zeta potential analyzer (Zeta Plus; Brookhaven Instruments Holtsville, NY, USA). For all experiments, the applied voltage and flow were started well before the sample was injected. The applied fields were typically square, had frequencies from 0.1 to 20 Hz, and were applied at voltages from 2 to 20 V peak-to-peak. The flow rate of the carrier was normally 1 mL/min.

3 Results and discussion

3.1 Electrical parameters

Figure 3 is a plot of the transient current response of an EIFFF system obtained when a 1 V step was applied for the three different carriers. Using a standard RC model, the electrical parameters of the channel were estimated as given in Table 1. These values are of the same order as those previously reported in the literature [21, 23].

Table 1. Measured values of electrical model components for carriers in the EIFFF channel

Carrier	R_B (Ω)	C_{DL} (F)	R_{DL} (Ω)
DI water	870	0.221	5882 Ω
5 μM Na_2CO_3	159	0.468	4545
50 μM Na_2CO_3	71.4	0.433	4500

Using the electrical parameter measurements for DI water, an estimate of the effective electric field that particles in the EIFFF channel would feel was made as a function of the frequency of the applied field as shown in

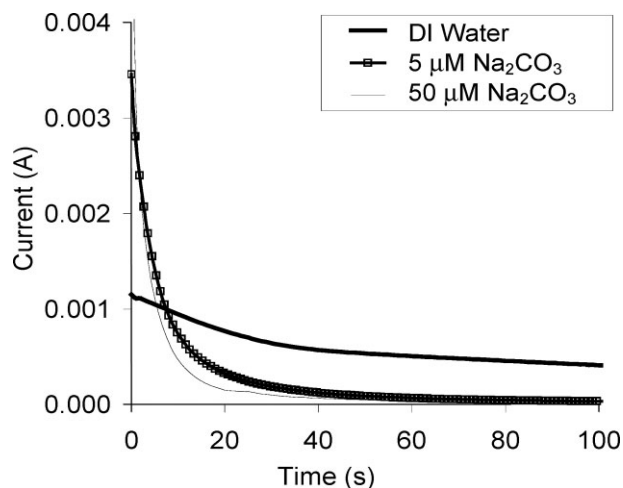


Figure 3. Current response for different carriers used in experiments when DC voltage is applied across the channel.

Fig. 4. The results of the parameter measurement and mathematical model indicate that even at low frequencies, the effective field should be nearly equal to the applied field. In fact the results indicate that larger systems will be more effective than smaller systems when using cyclical fields due to the slow development of the polarization layers. Microscale systems will also require higher frequencies to achieve cyclical separations than required in macroscale systems due to the rapid development of polarization layers in these tiny systems that devastate the effective electric field. In either case, the results suggest that the effective field in the channel should be nearly identical to the applied field and adjustments for the magnitude of the effective field in the model for Cy/EIFFF should not need to be made.

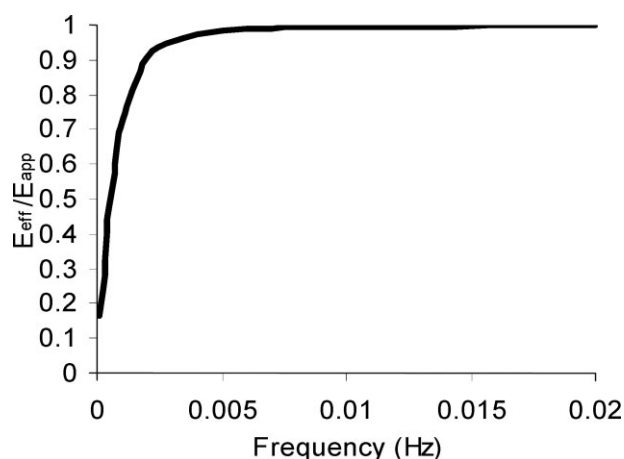


Figure 4. Estimate of effective field with frequency based on experimentally measured electrical parameters and Eq. (5).

3.2 Particle retention and separation

Knowing that electric fields experienced by particles in the EIFFF channel should be significant at even low frequencies, we began to perform basic retention experiments using polystyrene particles.

3.2.1 Mode I

Figure 5 is an overlay of fractograms for particles being retained in Mode I, obtained at varied voltages and with a constant frequency and flow rate. As the applied peak-to-peak voltage decreases from 20 V to 2 V, the elution times increase. This behavior is consistent with the theory for Cy/EIFFF systems operating in Mode I. Similar behavior can be obtained by maintaining the magnitude of the applied AC waveform and increasing the frequency of the applied voltage as shown in Fig. 6.

Early particle peaks: Examination of Fig. 5 reveals that an early peak (at about 130 s) occurs for each fractogram, and that this peak increases in size as λ_0 becomes very small. These peaks coincide with the void peak (elution time determined using acetone) and we speculate that they are caused by relatively unretained particles in the channel. The presence of this peak could cause a misconception that the analyte has two different types of particles or just passed off as a void peak. Changes in frequency, voltage, and electrophoretic mobility have no effect on the elution time of this peak. One potential reason these early peaks may exist is because there is no

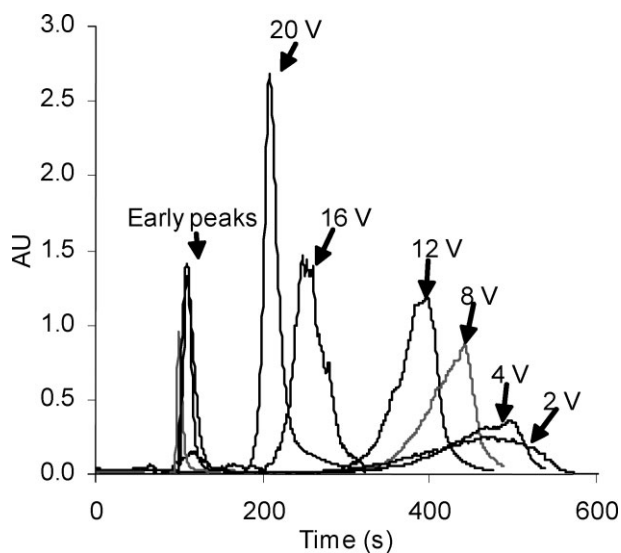


Figure 5. Fractograms for 100 nm polystyrene particles for different applied voltages operating in Mode I. The applied voltage is a square wave with a frequency of 3 Hz, while the carrier was $5\mu\text{M}$ Na_2CO_3 at 1 mL/min.

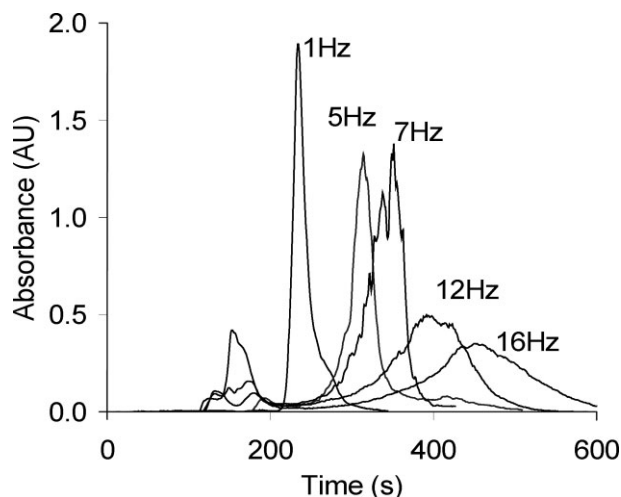


Figure 6. Fractograms for 160 nm polystyrene particles for different frequencies operating in Mode I. The applied voltage is a square wave with a magnitude of 20 V. The carrier was DI water at 1 mL/min.

relaxation of the sample before or during the analysis. Thus, particles initially occupy the full width of the channel. In Mode I, particles near one of the walls never come in contact with the wall, spend most of their time in fast flow lines, and accordingly elute with the void peak. Any particles that contact a wall synchronize with the others and move more slowly along the length of the channel. Thus, two groups of particles are generated and, accordingly, two particle peaks should be expected during mode I operation. The number of particles in the unretained group increases the smaller λ_0 becomes, since the total motion of particles decreases in the x -direction leaving more particles without any contact with a wall. Consequently, the quantity of particles contained in the void peak would and does increase as λ_0 decreases, and the observed early peak increases in area. Thus, the early peak is parasitic and reduces the number of particles retained as desired.

To combat the early peak, an offset voltage was applied throughout the analysis, and this method proved to successfully reduce or eliminate the peak, suggesting that the proposed hypothesis for the cause of the early peaks was correct. The offset voltage consistently nudges particles towards one of the walls, so particles in the middle of the channel eventually reach an oppositely charged electrode. A stop flow time to allow particles to migrate towards and accumulation wall also proved useful. A fractogram obtained using an offset voltage and stop flow period is shown in Fig. 7. Note the small early peak for a retention experiment that was normally consumed by the early peak and left no signal at the expected retention time. Compare with the data in Figs. 5 and 6.

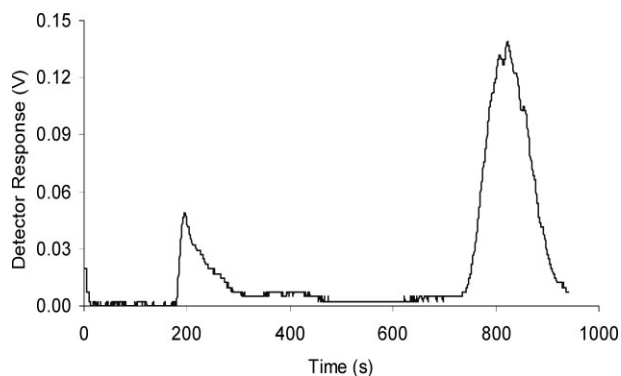


Figure 7. Reduction of the early particle peak using an offset voltage with 100 nm particles. A 6 Hz square wave of 4 V with a 1 V offset was applied ($\lambda_0 = 0.105$). DI water was the carrier at a flow rate of 1 mL/min. An 85 s stop flow period was employed.

3.2.2 Mode III

In Mode III, particles reach the opposite wall before the field is reversed. Figure 8 is an overlay of particle fractograms for different frequencies in Mode III. As predicted by the Cy/EIFFF models, elution times for particles in Mode III decrease as the frequency is increased. A similar effect can be obtained by increasing the applied voltage while in Mode III. Figure 8 also demonstrates that as frequency is decreased, the magnitude of the particle peaks is decreased and their width increased simultaneously, or the band broadening increased significantly.

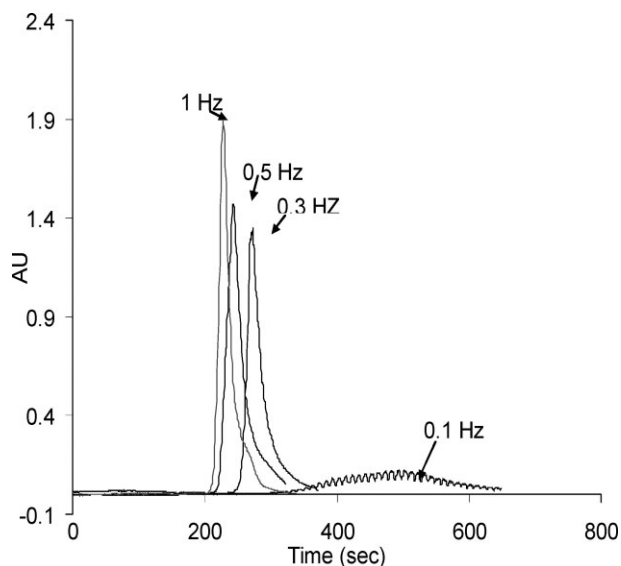


Figure 8. Fractograms for polystyrene particles of 160 nm diameter for different frequencies in Mode III. The voltage applied was a square wave with peak-to-peak amplitude of 20 V, and the carrier is DI water.

3.2.3 Band-broadening

This unwanted band-broadening decreases the resolution of a separation, so it is a critical performance measure in any chromatography system. In a Cy/EIFFF system, band-broadening increases as retention increases, creating a significant challenge. Plate height is a measure of band-broadening and was estimated from the collected data [24]. The results of these measurements are shown in Fig. 9, where the plate numbers, which correspond to fractionating power, are plotted as a function of λ_0 . Note that the plate numbers fall at both extreme high and low values of λ_0 , and that the maximum plate number occurs at a λ_0 of 0.284 rather than at the mode transition.

The causes of this band-broadening are not entirely clear. In Mode I, band-broadening seems to be caused by the different initial positions occupied by similar particles across the width of the channel, and by diffusion effects that are not considered in the models. Interactions with the wall appear to reduce band-broadening in Mode I, so band-broadening becomes more significant as λ_0 decreases. In Mode III, band-broadening appears to be primarily due to nonequilibrium and diffusion effects, which are promoted by high concentrations of the particles at the walls. Overall, band-broadening appears to be a significant challenge to successful implementation of CyEIFFF, as it grows rapidly with retention. We are working to determine the exact cause of this challenge, and to develop techniques for combating the problem. Preliminary indications are that offset voltages and changes in the ionic strength of the carrier may be used to combat band-broadening.

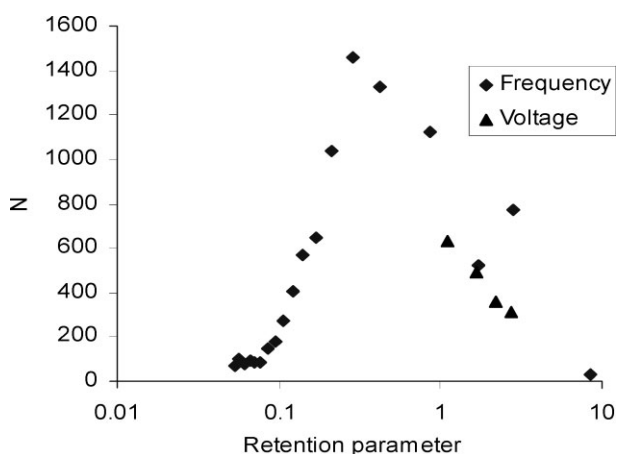


Figure 9. Plot of theoretical plates as a function of retention parameter, λ_0 , as frequency and voltage are varied. The voltage applied for the frequency runs is 20 V square wave and the flow rate was 0.9 mL/min. For the varying voltages, the frequency was 1 Hz and the flow rate was 1 mL/min. The carrier used was DI water.

3.2.4 Frequency effects on observed peaks

In Fig. 8 we note that a small, periodic oscillation is superimposed over the normal Gaussian peak, especially at very low frequencies. This periodic oscillation has a frequency identical to that for the applied field. The explanation for this effect is that during each cycle of the applied field, a few particles in the particle cloud move out of the channel, while other particles are retained or pulled back into the channel due to the reversal of the field. This event repeats itself with each cycle of the field creating an oscillatory particle concentration on top of the general particle concentration at the outlet, which is then reflected in the detector output. This effect becomes more pronounced as λ_0 increases.

3.2.5 Electrophoretic mobility effects

Electrophoretic mobility, μ , is the only parameter of the particles that should affect retention in a Cy/EIFFF system. The retention of particles that have a variety of electrophoretic mobilities follows similar trends to those presented for a variation in frequency and voltage with μ constant, so will not be expounded upon here. The primary point to remember is that particles will move from Mode I to Mode III as μ increases, as λ_0 is directly proportional to μ . Particles with different electrophoretic mobilities will instead be used to show both the power and

one of the complications of Cy/EIFFF systems. Figure 10 shows two pairs of fractograms involving the retention of particles of identical size, but with different mobilities. The first carboxylated polystyrene (PCA) particles have a measured μ of $9 \times 10^{-4} \text{ cm}^2/\text{V}\cdot\text{s}$ and the second carboxylated polystyrene (PCB) particles have a μ of $2 \times 10^{-4} \text{ cm}^2/\text{V}\cdot\text{s}$. In Fig. 10a, both the PCA and PCB particles elute at the same time, giving no resolution between them. Careful observation uncovers an early peak for the PCB particles and no early peak for the PCA particles. The early peak indicates that the PCB particles are in Mode I and the lack of one means that the PCA particles are in Mode III. Since the particles are in different modes, we should be able to pick a frequency where the separation of the particles would be optimized. Figure 10b shows the elution of the particles at a slightly higher frequency (3 Hz). In this case, since particles PCA were in Mode I, their elution time drops substantially. The PCB particles, since they were already in Mode I, increase their elution time (note the continued and increasing presence of an early peak). The difference between the elution times at this point is significant showing that careful manipulation of the operating conditions can tune a separation for optimal results. The reverse is also true, though, since an improper selection of operating conditions can set up a situation with little resolution. Accordingly, in Cy/EIFFF, unless the particles are already well-known, two analyses at different frequencies may be required to fully characterize the particles being examined and to eliminate possible confusion.

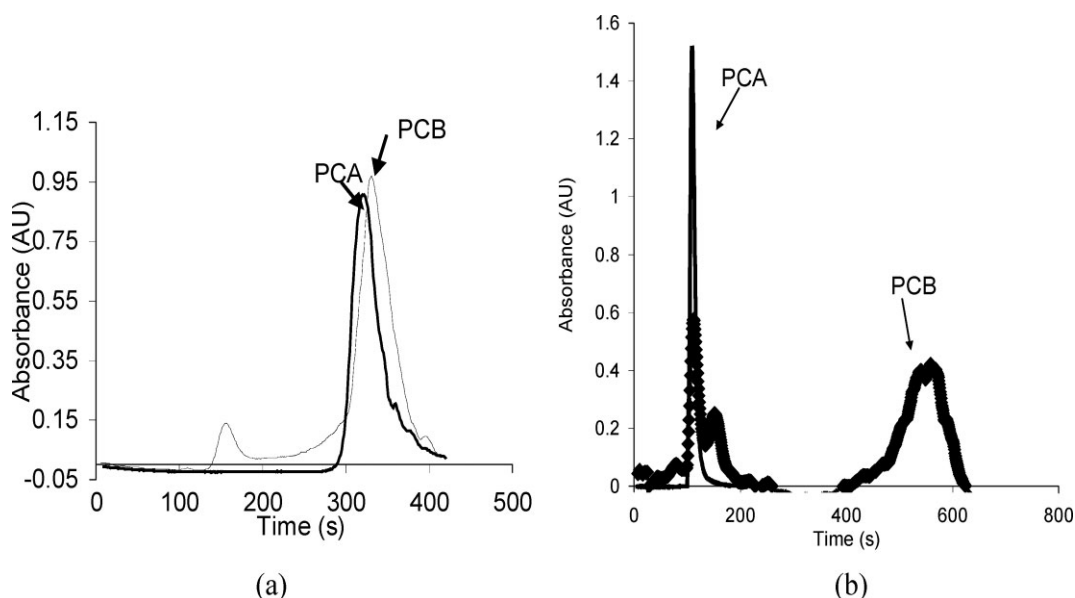


Figure 10. Fractograms for 160 nm polystyrene particles with $-\text{COOH}$ groups on the surface to give different electrophoretic mobilities. The conditions for both runs were an applied square wave of 20 V, a flow rate of 1 mL/min, and the carrier was $50 \mu\text{M Na}_2\text{CO}_3$ (a) 1 Hz (b) 3 Hz

3.2.6 Separation

A demonstration separation was performed using a mixture of 200 nm silica and 200 nm polystyrene particles as shown in Fig. 11. The elution time of the two particle types were determined in separate experiments by performing retention experiments under the same conditions used in Fig. 11 for both particles individually. Similar results were found for these particles using various frequencies, voltages, and flow rates. Separations with good resolution were found difficult to perform due to band-broadening issues as the highest retention ratios and the need to show retention of both populations of particles. The difficulty was found to be diminished by applying a small offset voltage and by providing a stop flow period to allow the particles to migrate towards one wall and synchronize. Combined, these two techniques seem to reduce early peaks while increasing resolution.

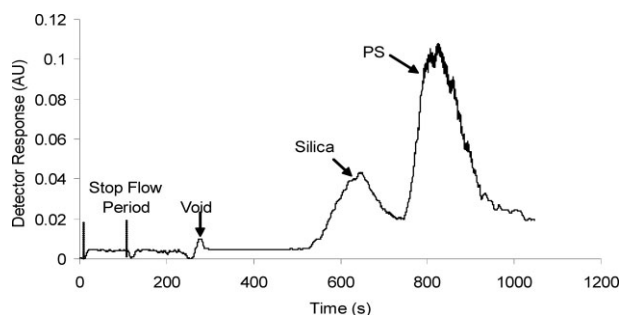


Figure 11. Fractogram showing separation of 200 nm silica particles from 200 nm polystyrene (PS) particles based on electrophoretic mobility. A 100 s stop flow period was used to allow particles to stabilize near one wall. An applied field of 10 VPP and 1 V offset at 5 Hz was used along with a carrier of DI water at 1 mL/min.

3.2.7 Flow rate

Experiments varying the flow rate (0.5–2.0 mL/min) were carried out to determine if changes in flow rate might have any unexpected effects on retention in Cy/EIFFF systems. The flow rate should not have any impact on retention, as the retention parameter is independent of flow rate. While the data is not published here, flow rate has little if any impact on the retention of particles in the channel and retention times followed the change in flow rate closely. Band-broadening also appeared to vary little over the range of flow rates examined [25].

3.2.8 Comparison to theory

Figure 12 illustrates the variation of elution time with λ_0 and compares the results to that predicted by theory. Both Modes I and III can be seen in the figure. The trends

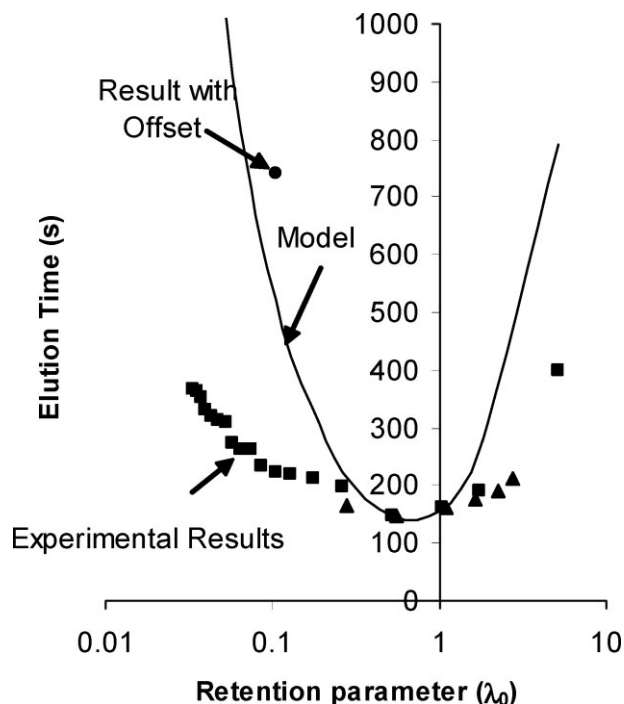


Figure 12. Variation of elution time with frequency (squares) and voltage (triangles) and plotted as a function of retention parameter. The data is the same as used in previous figures. The experimental results are corrected for the dead volume in the system.

in this plot match the basic theory for Cy/EIFFF, but the retention at low and high λ_0 values tends to be less than predicted. These results are significant in that previously published results using microscale systems did not follow these trends [12]. The deviation at high λ_0 values can possibly be attributed to the increasing importance of diffusion and the possible reappearance of polarization layers. Also, Giddings' theoretical models assume that once a particle reaches the wall, it stops moving along the length of the channel. This assumption fails due to both steric effects and diffusion effects, making modifications to the theory necessary.

A possible modification at high values of λ_0 might be to include the normal model for EIFFF once particles reach the opposite wall. Accordingly, the closest approach of particles could be estimated by the distance l , which is given by the equation

$$l = \frac{D}{\mu E_0} \quad (10)$$

where D is the diffusion coefficient of the particles. The primary complication of this approach is that E_0 is no longer a constant value, but varies according to the frequency of the applied field and the time the particles

reach the wall. Thus, I would be a function of both frequency and time, except in the case of a square wave, would be somewhat challenging to implement mathematically, and is beyond the scope of this work.

Another possible explanation for lower retention than predicted is that the magnitude of the effective electric field experienced by particles in the EIFFF channel might be less than predicted as the double layer reforms. This complication would likely be most significant at high values of λ_0 , but could be important depending on the type of channel in use and the associated electrical parameters in the system. Thus, further exploration of this possible adjustment to the mathematical models for the Cy/EIFFF system will be reserved for future communications.

Returning to Fig. 12 to examine the shortcomings of the model with respect to Mode I, the likely cause of retention loss is diffusion away from the wall. With nothing to keep particles near the wall, the retained particles will drift into fast flow lines and elution times will fall. This diffusion into the channel could be reduced by the use of an offset voltage, which was also discussed in relation to the reduction and elimination of early particle peaks. The single labeled data point on Fig. 12 represents a data point collected with an offset voltage (Fig. 7) showing a closer agreement to the models, but in this case the elution time is greater than predicted. The increase may be due to the particles eluting in a “normal” EIFFF mode, but the retention time is still higher than would be predicted for these particles if only normal EIFFF was being used [5, 6], so the combination of both cyclical and offset voltages may produce a more powerful system than either separately. Additional work will be required to determine the feasibility of such a system and the potential advantages. From a practical standpoint, an offset voltage may be required during Mode I operation to not only eliminate the presence of early particle peaks, but also to produce higher retention and better agreement with the mathematical models of the Cy/EIFFF channel. Another interesting feature to note in Fig. 12 is that the minimum elution time should occur for λ_0 equal to 0.75, which is very nearly the case here (no experiments were performed for a λ_0 of exactly 0.75), and the estimated retention times are more accurate in this region, suggesting that some features of the model are correct.

4 Concluding remarks

The primary conclusion of this work is that macroscale EIFFF channels can be used to perform Cy/EIFFF, and that they follow theoretical predictions more closely than do microscale systems. The improvement in macroscale systems compared to microscale systems is likely linked

to the relatively higher average currents (and associated fields) found in larger systems. Microscale systems fall to very low current levels rapidly, while larger systems have much larger time constants, and therefore maintain high currents for longer portions of the period of the applied field.

A secondary conclusion of this work is that Cy/EIFFF experiments follow the general trends predicted by theory, but do not always follow predictions well when operating at higher retention levels. The deviations from theory are likely associated with diffusion effects and lower effective electric fields than predicted. Thus, models that incorporate diffusion effects into the CyFFF theory need to be developed, and better models of the electric fields in the channel need to be applied to Cy/EIFFF. The operating conditions in the channel are important. The highly capacitive nature of the system turns out not to be a significant detriment to use of cyclical fields even at very low frequencies. While the results obtained using the system do not precisely agree with the theory presented for Cy/EIFFF across a broad range of operating conditions, the theory is predictive for operation of the system with λ_0 close to 1 and the overall trends are consistent. Methods to minimize discrepancies between the theory and experiment have been suggested and should improve the operation of the Cy/EIFFF system. The theory does accurately predict ranges for the important operating conditions in the Cy/EIFFF channel, such as voltage, waveform, frequency, and electrophoretic mobility, which makes implementation of Cy/EIFFF practical.

One question not addressed specifically in this work was the how Cy/EIFFF would work in EIFFF channels of smaller dimension, where field strengths would be increased dramatically. The results presented here point towards the success of this technique over a wide range of EIFFF channel sizes. Accordingly, work is ongoing to apply this technique to microscale FFF systems to develop a portable Cy/EIFFF system. On another front, since the particles most likely to be used in Cy/EIFFF are relatively small when compared to other cyclical FFF systems, steric effects are likely to be small and the operation of the system can be broken down into only two modes. With small particles, though, diffusion is more significant, so future work will need to better consider the effect that diffusion has on retention. Accordingly, particles with relatively low diffusion coefficients compared to their electrophoretic mobility may be ideal for analysis using Cy/EIFFF. Nucleic acids, including DNA, liposomes, viruses, and cells may all fit into this category.

As a newly demonstrated instrumental technique, the potential applications of Cy/EIFFF still need to be explored and developed. The ability to tune the system

and precisely separate particles based on small differences in electrophoretic mobility may prove to be the technique's most promising advantage, especially since current electrophoretic analysis systems do not typically combine high sensitivity to electrophoretic mobility, the ability to collect the analyzed particles after analysis, low cost, and gentle, flexible operating conditions. Finally, with the increasing emphasis on nanotechnology and a need for techniques that can characterize, sort, and manipulate nanoscale objects, Cy/EIFFF may find a role in nanomanufacturing. With the field of nanotechnology in the midst of a rapid expansion, this role is yet to be clearly defined.

Funding for this work was provided by NSF grant EPS-0092001 and the University of Utah. The authors would like to thank Karin Caldwell for generously providing the EIFFF instrument used during the experimental work.

Received November 3, 2004

5 References

- [1] Giddings, J. C., *Sep. Sci.* 1966, 1, 123–125.
- [2] Caldwell, K. D., Kesner, L. F., Meyers, M. N., Giddings, J. C., *Science* 1972, 176, 296–298.
- [3] Caldwell, K. D., Gao, Y. S., *Anal. Chem.* 1993, 65, 1764–1772.
- [4] Gale, B. K., Caldwell, K. D., Frazier, A. B., *IEEE Trans. Biomed. Eng.* 1998, 45, 1459–1469.
- [5] Tri, N., Caldwell, K. D., Beckett, R., *Anal. Chem.* 2000, 72, 1823–1829.
- [6] Gale, B. K., Caldwell, K. D., Frazier, A. B., *Anal. Chem.* 2002, 74, 1024–1030.
- [7] Chmelik, J., Deml, M., Janca, J., *Anal. Chem.* 1989, 61, 912.
- [8] Thormann, W., Firestone, M. A., Dietz, M. L., Ceceonie, T., Mosher, R. A., *J. Chromatogr.* 1989, 461, 95–101.
- [9] Chmelik, J., Thormann, W., *J. Chromatogr.* 1993, 632, 229–234.
- [10] Gale, B. K., Thoppil, M., in: *Proc. 9th Int. Symp. Field-Flow Fractionation*, Boulder, CO, June 26–29, 2001.
- [11] Srinivas, M., Gale, B. K., in: *Proc. 10th Int. Symp. Field-Flow Fractionation*, Amsterdam, The Netherlands, July 2–5, 2002.
- [12] Lao, A. I. K., Trau, D., Hsing, I. M., *Anal. Chem.* 2002, 74, 5364–5369.
- [13] Giddings, J. C., *Anal. Chem.* 1986, 58, 2052–2056.
- [14] Lee, S., Myers, M. N., Beckett, R., Giddings, J. C., *Anal. Chem.* 1988, 60, 1129–1135.
- [15] Stevens, F. J., *J. Biochem. Biophys. Methods* 1990, 20, 275–292.
- [16] Chandhok, A. K., Leighton, D. T., *AIChE J.* 1991, 37, 1537–1549.
- [17] Shapiro, M., Brenner, H., *Phys. Fluids* 1990, A2, 1731–1743.
- [18] Shapiro, M., Brenner, H., *Phys. Fluids* 1990, A2, 1744–1753.
- [19] Mollay, R. F., Gallagher, C. T., Leighton, D. T., *NASA Conf. Pub.* 1996, 3338, 723–728.
- [20] Shmidt, J. L., Cheh, H. Y., *Sep. Sci. Tech.* 1990, 25, 889–902.
- [21] Palkar, S. A., Schure, M. R., *Anal. Chem.* 1997, 69, 3223–3229.
- [22] Gale, B. K., Caldwell, K. D., Frazier, A. B., *Anal. Chem.* 2001, 73, 2345–2352.
- [23] Bard, A. J., Faulkner, L. R., *Electrochemical Methods: Fundamentals and Applications*, Wiley, New York 2000.
- [24] Said, A. S., *Theory and Mathematics of Chromatography*, Dr. Alfred Huethig Publishers, Heidelberg, Germany 1981.
- [25] Srinivas, M., Masters Thesis, available at <http://www.mem-s.utah.edu/Theses/Meregu%20Complete%20Thesis.pdf>. 2002.